PHYSICAL REVIEW D **93,** 065049 (2016)

Aharonov-Bohm phases in a quantum LC circuit

ChunJun Cao,[1] Yuan Yao,[2] and Ariel R. Zhitnitsky[2]
[1]*Walter Burke Institute for Theoretical Physics, California Institute of Technology, Pasadena, California 91125, USA*
[2]*Department of Physics and Astronomy, University of British Columbia, Vancouver, British Columbia V6T 1Z1, Canada*
(Received 14 December 2015; published 23 March 2016)

We study novel types of contributions to the partition function of the Maxwell system defined on a small compact manifold. These contributions, often not addressed in the perturbative treatment with physical photons, emerge as a result of tunneling transitions between topologically distinct but physically identical vacuum winding states. These new terms give an extra contribution to the Casimir pressure, yet to be measured. We argue that this effect is highly sensitive to a small external electric field, which should be contrasted with the conventional Casimir effect, where the vacuum photons are essentially unaffected by any external field. Furthermore, photons will be emitted from the vacuum in response to a time-dependent electric field, similar to the dynamical Casimir effect in which real particles are radiated from the vacuum due to the time-dependent boundary conditions. We also propose an experimental setup using a quantum LC circuit to detect this novel effect. We expect physical electric charges to appear on the capacitor plates when the system dimension is such that coherent Aharonov-Bohm phases can be maintained over macroscopically large distances.

DOI: 10.1103/PhysRevD.93.065049

I. INTRODUCTION: MOTIVATION

It has been recently argued [1–4] that some novel terms in the partition function emerge when a pure Maxwell theory is defined on a small compact manifold. These terms are not related to the propagating photons with two transverse physical polarizations, which are responsible for the conventional Casimir effect (CE) [5]. Rather, they occur as a result of tunneling events between topologically different but physically identical $|k\rangle$ topological sectors. While such contributions are trivial in Minkowski space-time $\mathbb{R}_{1,3}$, they become important when the system is defined on certain small compact manifolds. Without loss of generality, consider a manifold $\mathbb{M}$ which has at least one nontrivial direct factor of the fundamental group, e.g., $\pi_1[U(1)] \cong \mathbb{Z}$. The topological sectors $|k\rangle$, which play a key role in our discussions, arise precisely from the presence of such nontrivial mappings for the Maxwell $U(1)$ gauge theory. The corresponding physically observable phenomenon has been termed the topological Casimir effect (TCE).

In particular, it has been explicitly shown in [1] that these novel terms in the topological portion of the partition function $\mathcal{Z}_{\rm top}$ lead to a fundamentally new contribution to the Casimir vacuum pressure that appears as a result of tunneling events between topological sectors $|k\rangle$. Furthermore, $\mathcal{Z}_{\rm top}$ displays many features of topologically ordered systems, which were initially introduced in the context of condensed matter systems (see recent reviews [6–10]): $\mathcal{Z}_{\rm top}$ demonstrates the degeneracy of the system, which can only be described in terms of nonlocal operators [2]; the infrared physics of the system can be studied in terms of nonpropagating auxiliary topological fields [3], analogous to how a topologically ordered system can be analyzed in terms of Berry's connection (also an emergent rather than fundamental field), and the corresponding expectation value of the auxiliary topological field determines the phase of the system. Finally, one can show [4] that if the same system is placed in a time-dependent magnetic field $B^z_{\rm ext}(t)$, real photons will be emitted from the vacuum, similar to the so-called dynamical Casimir effect (DCE) [11–13]. The difference from the conventional DCE is that the dynamics of the vacuum in our system defined on a small compact manifold is not related to the fluctuations of the conventional degrees of freedom, the virtual photons. Rather, the radiation here arises from tunneling events between topologically different but physically identical $|k\rangle$ sectors in a time-dependent background.

As we review in Sec. II, the relevant vacuum fluctuations which saturate the topological portion of the partition function $\mathcal{Z}_{\rm top}$ are formulated in terms of topologically nontrivial boundary conditions. Classical instantons formulated in Euclidean space-time satisfy the periodic boundary conditions up to a large gauge transformation and provide a topological magnetic instanton flux in the z direction. These integer magnetic fluxes describe the tunneling transitions between physically identical but topologically distinct $|k\rangle$ sectors. Precisely these field configurations generate an extra Casimir vacuum pressure in the system. What happens to this complicated vacuum structure when the system is placed in the background of a constant external magnetic field $B^z_{\rm ext}$? The answer is known [1]: the corresponding partition function $\mathcal{Z}_{\rm top}$ as well as all observables, including

the topological contribution to the Casimir pressure, are highly sensitive to small magnetic fields and demonstrate 2π periodicity with respect to magnetic flux represented by the parameter $\theta_{\rm eff} \equiv eSB^z_{\rm ext}$, where S is the xy area of the system $\mathbb{M}$. This sensitivity to an external magnetic field is a result of the quantum interference of the external field with the topological quantum fluctuations. Alternatively, one can see this as resulting from a small but nontrivial overlap between the conventional Fock states, constructed by perturbative expansions around each $|k\rangle$ sector, and the true energy eigenstates of the theory, which are only attainable in a nonperturbative computation that takes the tunneling into account. This strong "quantum" sensitivity of the TCE should be contrasted with conventional Casimir forces, which are practically unaltered by any external field due to the strong suppression $\sim B^2_{\rm ext}/m^4_e$ (see [1] for the details).

The main goal of the present work is to study the dynamics of electric instanton fluxes, in contrast to the magnetic ones considered previously in [1–4]. Placing metallic plates at the opposing ends in the z direction endows our system with the geometry of a small quantum capacitor. Periodic boundary conditions up to a large gauge transformation can be enforced by connecting the two plates of the capacitor with an external wire. Thus, the system forms a quantum LC circuit where the wire provides the inductance. Formal computation of the partition function with electric-type instantons is very similar to previous studies. Like their magnetic counterparts, these electric instantons also describe tunneling transitions between physically identical but topologically distinct $|k\rangle$ sectors in Euclidean space-time. Both types of instanton fluxes give rise to an extra repulsive pressure, the opposite of the conventional CE, and both exhibit oscillatory behavior in pressure, induced field, and susceptibility in response to an external field represented by an effective theta parameter, $\theta_{\rm eff}$.

However, the behavior of the system as well as the physical interpretation drastically changes when one considers the system placed in an external field: while the magnetic field in space-time with Euclidean or Minkowski signatures remains unaltered, the electric fluxes pick up an imaginary i in the transition from Minkowski to Euclidean space-time. Most notably, whereas the magnetic oscillations have universal 2π periodicity for all system sizes, the periodicity in the electric system varies with the system size. Compared to the magnetic system, an advantage of the electric system is that the system size can be much more easily optimized to produce topological effects of order one.

The topological instanton configurations which describe the tunneling transitions are formulated in terms of periodic boundary conditions on the gauge field up to a large gauge transformation. These boundary conditions correspond to persistent fluctuating charges that reside on the capacitor plates. These charges can be interpreted as a consequence of the Aharonov-Bohm phases of the topological vacuum. Positive and negative charges on each plate cancel exactly in the absence of an external electric field, but with a nonvanishing external field, each plate acquires a nonzero net charge, giving rise to an induced dipole moment.

We also study the emission of real photons from the topological vacuum when the external electric field varies slowly (in the adiabatic limit). The external field interferes with the topological vacuum configurations and generates real photons whose energy ultimately comes from the time-varying external field. One can also explain this emission in terms of the dipole moment generated by the fluctuating electric charges. As the external field takes on time dependence, so does the induced dipole moment. And a time-varying dipole moment naturally implies electromagnetic radiation.

The structure of our presentation is as follows. In Sec. II, we review the construction of magnetic-type instantons and the partition function $\mathcal{Z}_{\rm top}$ in [1–4]. We also explain how an external magnetic field enters $\mathcal{Z}_{\rm top}$. In Sec. III, we construct the electric-type instantons that are the focus of the present studies, and their extra vacuum energy contribution. In Sec. IV, we consider the system placed in an external electric field. In particular, we explain in detail how to correctly treat an external field applied in Minkowski space-time in the Euclidean description. We also compute the various physical parameters of the system such as the induced electric field and corresponding susceptibility which measures the response of the system with respect to the applied field. In Sec. V, we provide an alternative interpretation of the topological vacuum configurations in terms of fluctuating boundary charges, and comment on the connection with a previously discussed phenomenon of persistent currents. In Sec. VI we propose an experimental setup using quantum LC circuits to detect these topological effects, and numerically estimate the magnitude of the boundary charges and the associated dipole moment in systems with experimentally accessible dimensions. In Sec. VII we discuss the emission of real photons as the static external field takes on time dependence. And in Sec. VIII, we conclude the present studies and speculate on the possible relevance of the TCE for cosmology. In particular, the de Sitter behavior in the inflationary epoch could be an inherent property of the topological sectors in QCD in the expanding Universe, rather than a result of some *ad hoc* dynamical field such as inflaton. The emission of real physical degrees of freedom from the inflationary vacuum in a time-dependent background (the so-called reheating epoch) in all respects resembles the effect considered in the present work where real photons can be emitted from the vacuum in a time-varying external electric field.

II. TOPOLOGICAL PARTITION FUNCTION: MAGNETIC-TYPE INSTANTONS

Our goal here is to review the Maxwell system defined on a Euclidean 4-torus with sizes $L_1 \times L_2 \times L_3 \times \beta$ in the

respective directions. This 4-torus provides the infrared regularization of the system, which plays a key role in the proper treatment of the topological terms related to tunneling events between topologically distinct but physically identical $|k\rangle$ sectors.

We follow [1] in our construction of the partition function $\mathcal{Z}_{\rm top}$, where it was employed to compute the corrections to the Casimir effect due to these topological fluctuations. The crucial point is that we impose periodic boundary conditions on the gauge field A^μ up to a large gauge transformation. In what follows we simplify our analysis by considering a clear case with winding topological sectors $|k\rangle$ in the z direction only. The classical instanton configuration in Euclidean space which describes the corresponding tunneling transitions can be represented as follows:

$$A^\mu_{\rm top} = \left(0, -\frac{\pi k}{eL_1L_2}x_2, \frac{\pi k}{eL_1L_2}x_1, 0\right), \tag{1}$$

where k is the winding number that labels the topological sector, and L_1, L_2 are the dimensions of the plates in the x and y directions respectively, assumed to be much larger than the plate separation in the z direction, L_3. The terminology "instanton" is adapted from similar studies in 2D QED [1], where the corresponding configuration in the $A_0 = 0$ gauge describes the interpolation between pure gauge vacuum winding states $|k\rangle$. We use the same terminology and interpretation for the 4D case because (2) is the classical configuration saturating the partition function $\mathcal{Z}_{\rm top}$, in close analogy with the 2D case (details in [1]). This classical instanton configuration satisfies the periodic boundary conditions up to a large gauge transformation, and provides a topological magnetic instanton flux in the z direction:

$$\vec{B}_{\rm top} = \vec{\nabla}\times\vec{A}_{\rm top} = \left(0, 0, \frac{2\pi k}{eL_1L_2}\right),$$
$$\Phi = e\int dx_1 dx_2 B^z_{\rm top} = 2\pi k. \tag{2}$$

The Euclidean action of the system is quadratic and has the form

$$\frac{1}{2}\int \mathrm{d}^4x\{\vec{E}^2 + (\vec{B}+\vec{B}_{\rm top})^2\}, \tag{3}$$

where $\vec{E}$ and $\vec{B}$ are the dynamical quantum fluctuations of the gauge field. We call the configuration given by Eq. (1) the instanton fluxes describing the tunneling events between topological sectors $|k\rangle$. These configurations saturate the partition function [see (6) below] and should be interpreted as "large" quantum fluctuations which change the winding states $|k\rangle$, in contrast to "small" quantum fluctuations, which are topologically trivial and are expressed in terms of conventional virtual photons saturating the quantum portion of the partition function $\mathcal{Z}_{\rm quant}$.

The key point is that the topological portion $\mathcal{Z}_{\rm top}$ decouples from the quantum fluctuations, $\mathcal{Z} = \mathcal{Z}_{\rm quant}\times\mathcal{Z}_{\rm top}$, such that the quantum fluctuations do not depend on topological sectors $|k\rangle$ and can be computed in the trivial topological sector, $k = 0$. Indeed, the cross term vanishes,

$$\int \mathrm{d}^4x\vec{B}\cdot\vec{B}_{\rm top} = \frac{2\pi k}{eL_1L_2}\int \mathrm{d}^4x B_z = 0, \tag{4}$$

because the magnetic portion of the quantum fluctuations in the z direction, represented by $B_z = \partial_x A_y - \partial_y A_x$, is a periodic function, as $\vec{A}$ is periodic over the domain of integration. This technical remark in fact greatly simplifies our analysis as the contribution of the physical propagating photons is not sensitive to the topological sectors. This is, of course, a specific feature of quadratic action (3), in contrast to non-Abelian and nonlinear gauge field theories where quantum fluctuations do depend on the topological sectors.

The classical action for configuration (2) then takes the form

$$\frac{1}{2}\int \mathrm{d}^4x\vec{B}^2_{\rm top} = \frac{2\pi^2k^2\beta L_3}{e^2L_1L_2}. \tag{5}$$

To further simplify our analysis in computing $\mathcal{Z}_{\rm top}$, we consider a geometry where $L_1, L_2 \gg L_3, \beta$, similar to the construction of the conventional CE. In this case our system is closely related to 2D Maxwell theory by dimensional reduction: taking a slice of the 4D system in the xy plane will yield precisely the topological features of the 2D torus considered in great detail in [1]. Furthermore, with this geometry our simplification (2), where we consider exclusively the magnetic instanton fluxes in the z direction is justified, as the corresponding classical action (5) assumes a minimum possible value. With this assumption we can consider very low temperatures, but still we cannot take the formal limit $\beta\to\infty$ in the final expressions because of the technical constraints.

With these additional simplifications the topological partition function becomes

$$\mathcal{Z}_{\rm top} = \sqrt{\frac{2\pi\beta L_3}{e^2L_1L_2}}\sum_{k\in\mathbb{Z}} e^{-\frac{2\pi^2k^2\beta L_3}{e^2L_1L_2}} = \sqrt{\pi\tau}\sum_{k\in\mathbb{Z}} e^{-\pi^2\tau k^2}, \tag{6}$$

where we have introduced the dimensionless system size parameter

$$\tau \equiv 2\beta L_3/e^2L_1L_2. \tag{7}$$

Equation (6) is essentially the dimensionally reduced expression of the topological partition function for the

2D Maxwell theory analyzed in [1]. One should also note that the normalization factor $\sqrt{\pi\tau}$ which appears in (6) does not depend on the topological sectors $|k\rangle$, and essentially represents our normalization convention $\mathcal{Z}_{\rm top} \to 1$ in the limit $L_1 L_2 \to \infty$, which corresponds to a convenient setup for Casimir-type experiments. The simplest way to demonstrate that $\mathcal{Z}_{\rm top} \to 1$ in the limit $\tau \to 0$ is to use the dual representation (10), see below.

Next, we introduce an external magnetic field to the Euclidean Maxwell system. Normally, in the conventional quantization of electromagnetic fields in infinite Minkowski space, there is no *direct* coupling between the fluctuating vacuum photons and an external magnetic field due to the linearity of the Maxwell equations. Coupling with fermions generates a negligible effect $\sim\alpha^2 B^2_{\rm ext}/m_e^4$, as the nonlinear Euler-Heisenberg effective Lagrangian suggests (see [1] for the details and numerical estimates). In contrast, the external magnetic field does couple with the topological fluctuations (2) and can lead to effects of order unity.

The corresponding partition function can be easily constructed for the external magnetic field $B^z_{\rm ext}$ pointing along the z direction, as the crucial decoupling of the background field from the quantum fluctuations assumes the same form (4). In other words, the physical propagating photons with nonvanishing momenta are not sensitive to the topological sectors $|k\rangle$, nor to the external magnetic field, similar to the discussions after Eq. (4). Additionally, since a real-valued external magnetic field applied in Minkowski space-time remains the same after analytic continuation to Euclidean space-time, this $B^z_{\rm ext}$ can be used to represent both the Minkowski external field and the Euclidean one.

The classical action in the presence of this uniform static magnetic field $B^z_{\rm ext}$ therefore takes the form

$$\frac{1}{2}\int {\rm d}^4x(\vec{B}_{\rm ext}+\vec{B}_{\rm top})^2 = \pi^2\tau\left(k+\frac{\theta_{\rm eff}}{2\pi}\right)^2, \qquad (8)$$

where the effective theta parameter $\theta_{\rm eff} \equiv eL_1L_2B^z_{\rm ext}$ is defined in terms of the external magnetic field $B^z_{\rm ext}$. And the partition function can be easily reconstructed from (6):

$$\mathcal{Z}_{\rm top}(\tau,\theta_{\rm eff}) = \sqrt{\pi\tau}\sum_{k\in\mathbb{Z}}\exp\left[-\pi^2\tau\left(k+\frac{\theta_{\rm eff}}{2\pi}\right)^2\right]. \qquad (9)$$

The dual representation for the partition function is obtained by applying the Poisson summation formula such that (9) becomes

$$\mathcal{Z}_{\rm top}(\tau,\theta_{\rm eff}) = \sum_{n\in\mathbb{Z}}\exp\left[-\frac{n^2}{\tau}+{\rm i}n\cdot\theta_{\rm eff}\right]. \qquad (10)$$

Equation (10) justifies our notation for the effective theta parameter $\theta_{\rm eff}$ as it enters the partition function in combination with integer n. One should emphasize that the n in the dual representation (10) is not the integer magnetic flux k defined in Eq. (2) which enters the original partition function (6). Furthermore, the $\theta_{\rm eff}$ parameter which enters (9), (10) is not the fundamental θ parameter normally introduced into the Lagrangian in front of the $\vec{E}\cdot\vec{B}$ operator. Rather, $\theta_{\rm eff}$ should be understood as an effective parameter representing the construction of the $|\theta_{\rm eff}\rangle$ state for each slice with nontrivial $\pi_1[U(1)]$ in the 4D system. In fact, there are three such $\theta^{M_i}_{\rm eff}$ parameters representing different slices of the 4-torus and their corresponding external magnetic fluxes. There are similarly three $\theta^{E_i}_{\rm eff}$ parameters representing the external electric fluxes (in Euclidean space-time) as discussed in [2] and as we will discuss in Sec. IV, such that the total number of θ parameters classifying the system is 6, in agreement with the total number of hyperplanes in four dimensions.[1]

We shall not elaborate on this classification in the present work. Instead, we limit ourselves to a single $\theta^{E_z}_{\rm eff}$ describing the partition function in the presence of a (Euclidean) external electric field $E^z_{\rm ext}$ pointing in the z direction. So essentially in what follows, we consider the manifold $\mathbb{I}^1\times\mathbb{I}^1\times\mathbb{S}^1\times\mathbb{S}^1$, where $\mathbb{I}^1$ is an interval in the x and y directions with length L_1 and L_2 respectively, while a single spatial circle $\mathbb{S}^1$ with size L_3 points in the z direction. Later in the paper, we interpret the obtained results by switching back to the physical Minkowski space-time. As we shall see, there are significant differences in the behavior of the system in comparison with the previously considered magnetic case [1].

III. ELECTRIC-TYPE INSTANTONS

We formulate the electric system on a Euclidean 4-manifold $\mathbb{I}^1\times\mathbb{I}^1\times\mathbb{S}^1\times\mathbb{S}^1$ with size $L_1\times L_2\times L_3\times\beta$. Two parallel conducting plates form the boundary in the z direction, endowing the system with the geometry of a small quantum capacitor that has plate area $L_1\times L_2$ and separation L_3 at an ambient temperature of $T=1/\beta$. These two plates are connected by an external wire to enforce the periodic boundary conditions (up to large gauge transformations) in the z direction, and so the system can be viewed as a quantum LC circuit where the external wire forms an inductor L. The quantum vacuum between the plates (where the tunneling transitions occur) represents the object of our studies.

A. Construction of topological partition function

The classical instanton configuration in Euclidean space-time which describes tunneling transitions between the topological sectors $|k\rangle$ can be represented as follows:

[1]Since it is not possible to have a 3D spatial torus without embedding it in 4D spatial space, the corresponding construction where all six possible types of fluxes are generated represents a purely academic interest.

$$A^{\mu}_{\rm top}(t) = \left(0, 0, 0, \frac{2\pi k}{eL_3\beta}t\right)$$
$$A^{3}_{\rm top}(\beta) = A^{3}_{\rm top}(0) + \frac{2\pi k}{eL_3}, \tag{11}$$

where k is the winding number that labels the topological sector and t is the Euclidean time. This classical instanton configuration satisfies the periodic boundary conditions up to a large gauge transformation, and produces a topological electric instanton flux in the z direction:

$$\vec{E}_{\rm top} = \dot{\vec{A}}_{\rm top} = \left(0, 0, \frac{2\pi k}{eL_3\beta}\right). \tag{12}$$

This construction of these electric-type instantons is in fact much closer (in comparison with the magnetic instantons discussed in [1]) to the Schwinger model on a circle where the relevant instanton configurations were originally constructed [14]. The Euclidean action of the system takes the form

$$\frac{1}{2}\int {\rm d}^4x\{(\vec{E} + \vec{E}_{\rm top})^2 + \vec{B}^2\}, \tag{13}$$

where, as in the magnetic case, $\vec{E}$ and $\vec{B}$ are the dynamical quantum fluctuations of the gauge field. Because periodic boundary conditions have been imposed on the system, the topological and quantum portions of the partition function again decouple: $\mathcal{Z} = \mathcal{Z}_{\rm quant} \times \mathcal{Z}_{\rm top}$. One can explicitly check that the cross term vanishes:

$$\int {\rm d}^4x \vec{E}\cdot\vec{E}_{\rm top} = \frac{2\pi k}{e\beta L_3}\int {\rm d}^4x E_z = 0, \tag{14}$$

since $E_z = \partial_0 A_z - \partial_z A_0$ and $\vec{A}$ is periodic over the domain of integration. Hence, the classical action for configuration (11) becomes

$$\frac{1}{2}\int {\rm d}^4x \vec{E}^2_{\rm top} = \frac{2\pi^2k^2L_1L_2}{e^2L_3\beta} = \pi^2k^2\eta, \tag{15}$$

where η is the key parameter characterizing the size of this electric system, defined as

$$\eta \equiv \frac{2L_1L_2}{e^2\beta L_3}. \tag{16}$$

This dimensionless parameter is related to the τ parameter in the magnetic case (7) by $\eta = 4/e^4\tau$. With topological action (15), we next follow the same procedure as in the magnetic case to construct the topological partition function,

$$\mathcal{Z}_{\rm top}(\eta) = \sum_{k\in\mathbb{Z}} e^{-\pi^2\eta k^2}, \tag{17}$$

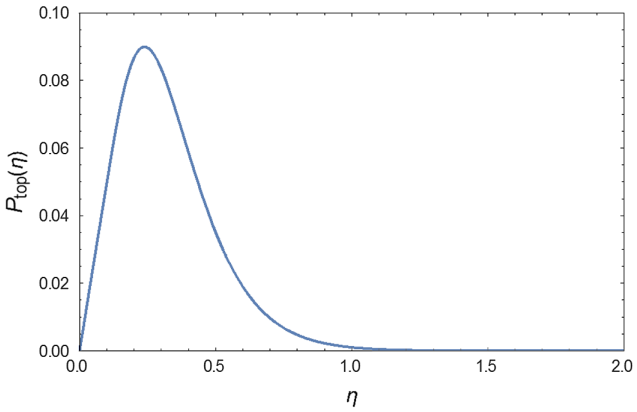

FIG. 1. A numerical plot of the topological Casimir pressure as a function of the system size parameter $\eta = 2L_1L_2/e^2\beta L_3$. Maximum pressure is observed at $\eta \approx 0.25$. Here the pressure is shown in units of $e^2/2L_1^2L_2^2$.

with normalization $\mathcal{Z}_{\rm top}(\eta \to \infty) = 1$, such that no topological effect survives in the limit $L_1L_2 \to \infty$. As a result, Eq. (17) differs from the partition function in the magnetic case (17) by a k-independent prefactor. Since the total partition function is represented by the direct product, $\mathcal{Z} = \mathcal{Z}_{\rm quant} \times \mathcal{Z}_{\rm top}$, any k-independent factor in the normalization of $\mathcal{Z}_{\rm top}$ can be moved to $\mathcal{Z}_{\rm quant}$.

The Poisson summation formula can be invoked to obtain the dual expression for the partition function:

$$\mathcal{Z}_{\rm top}(\eta) = \frac{1}{\sqrt{\pi\eta}}\sum_{n\in\mathbb{Z}} e^{-\frac{n^2}{\eta}}. \tag{18}$$

B. Topological Casimir pressure

The topological pressure between the capacitor plates can be obtained by differentiating the free energy of the system with respect to plate separation. First, we consider the pressure in the absence of an external electric field:

$$P_{\rm top}(\eta) = \frac{1}{\beta L_1L_2}\frac{\partial}{\partial L_3}\ln \mathcal{Z}_{\rm top}(\eta)$$
$$= \frac{e^2}{2L_1^2L_2^2}\frac{\pi^2\eta^2}{\mathcal{Z}_{\rm top}(\eta)}\sum_{k\in\mathbb{Z}} k^2 e^{-\pi^2\eta k^2}, \tag{19}$$

plotted in Fig. 1 as a function of the system size parameter η. The pressure peaks around $\eta \approx 0.25$ and has a narrower window compared to the magnetic case [1]. And like in the magnetic case, this pressure is repulsive, the opposite of the attractive conventional Casimir pressure. In the large η limit one can keep only two terms in expression (19) with $k = \pm 1$, and the pressure reduces to

$$P_{\rm top} \approx \frac{e^2\pi^2\eta^2}{L_1^2L_2^2}e^{-\pi^2\eta}, \tag{20}$$

with the familiar exponential suppression $\exp[-1/e^2]$ representing the typical behavior of tunneling processes.

To get a sense of the magnitude of this topological pressure, we compare it to the well-known expression for the conventional Casimir pressure between two parallel conducting plates with separation L_3:

$$P = -\frac{\pi^2}{240 L_3^4}. \tag{21}$$

From Fig. 1, the maximum topological pressure (corresponding to $\eta \approx 0.25$) is about $P_{\rm top}^{\rm max} \approx 0.1 e^2/2L_1^2L_2^2$, so the maximum ratio between the two pressures is

$$R_{\rm max} = \frac{|P_{\rm top}^{\rm max}|}{|P|} \approx \frac{12 e^2 L_3^4}{\pi^2 L_1^2 L_2^2} = \frac{48\alpha}{\pi}\frac{L_3^4}{L_1^2 L_2^2}. \tag{22}$$

This ratio, even at its maximum, is very small in a typical Casimir experiment setup where $L_1, L_2 \gg L_3$; besides, the numerical prefactor further suppresses it by an order of magnitude.

To sum up this section, we have found an additional contribution to the Casimir pressure that cannot be attributed to any physical propagating degrees of freedom but instead results from the topological excitation of the gauge field. Specifically, this contribution occurs when the system is defined on a compact manifold with nontrivial boundary conditions. As these topological tunneling transitions are described in terms of integer electric fluxes in Euclidean space-time (12), they exhibit exponential suppression in the conventional geometry, $\eta \to \infty$ (20). And even at its maximum, this topological pressure is orders of magnitude smaller than the conventional Casimir pressure (22). However, we show in the next section that a unique feature of the topological effect is that an external electric field effectively couples with the electric instanton fluxes (12), making the topological effect highly sensitive to an applied electric field. Similar sensitivity to external fields is absent from the conventional CE, where the linearity of the Maxwell equations forbids vacuum photon fluctuations from coupling to external fields.

IV. θ VACUA AND EXTERNAL ELECTRIC FIELDS

As shown in the previous section, the pressure produced by the topological CE is many orders of magnitude smaller than the conventional Casimir pressure, making its measurement very difficult. We know that in the magnetic case, as reviewed in Sec. II, a weak external magnetic field interferes with the integer magnetic fluxes describing the tunneling events (2) and enters the partition function (9), (10) as an effective theta parameter, eventually producing oscillatory behavior in the physical observables [1]. In this section, we consider the effect of similarly placing the quantum capacitor in a uniform external electric field in the z direction. However, whereas a magnetic field stays unchanged under analytic continuation between Minkowski and Euclidean formulations, an electric field acquires an additional factor of i as it involves the zeroth component of four-vectors, i.e., $E_z = \partial_0 A_z - \partial_z A_0$.

First we consider an external electric field in Euclidean space-time, which simply adds an $\vec{E}_{\rm ext}$ term to the topological action (15). Note that the quantum fluctuations still decouple from the topological and external fields due to the periodicity of the former over the domain of integration:

$$\left(E_{\rm ext}^z + \frac{2\pi k}{e\beta L_3}\right)\int {\rm d}^4 x E_z = 0. \tag{23}$$

The partition function then becomes

$$\mathcal{Z}_{\rm top}(\eta, \theta_{\rm eff}^E) = \sum_{k\in\mathbb{Z}} \exp\left[-\pi^2\eta\left(k + \frac{\theta_{\rm eff}^E}{2\pi}\right)^2\right], \tag{24}$$

where the external Euclidean electric field enters the partition function through the combination

$$\theta_{\rm eff}^E = e L_3 \beta E_{\rm ext}. \tag{25}$$

In what follows we also need a normalization at a nonvanishing external field. Since the portion of the partition function proportional to $E_{\rm ext}^2$ is also k independent, we move it to $\mathcal{Z}_{\rm quant}$. To avoid confusion with notation we use $\bar{\mathcal{Z}}_{\rm top}(\eta, \theta_{\rm eff}^E)$ for the partition function with this term removed. It is likewise normalized to one in the large η limit in the background of a nonvanishing external source, i.e.,

$$\begin{aligned}
\mathcal{Z}_{\rm top}(\eta, \theta_{\rm eff}^E) &\equiv \exp\left[-\frac{\eta(\theta_{\rm eff}^E)^2}{4}\right] \times \bar{\mathcal{Z}}_{\rm top}(\eta, \theta_{\rm eff}^E) \\
\bar{\mathcal{Z}}_{\rm top}(\eta, \theta_{\rm eff}^E) &\equiv \sum_{k\in\mathbb{Z}} \exp\left[-\pi^2\eta\left(k^2 + \frac{k\theta_{\rm eff}^E}{\pi}\right)\right] \\
\bar{\mathcal{Z}}_{\rm top}(\eta \to \infty, \theta_{\rm eff}^E) &= 1.
\end{aligned} \tag{26}$$

One can interpret $\bar{\mathcal{Z}}_{\rm top}(\eta, \theta_{\rm eff}^E)$ as the partition function with the external source contribution $\frac{1}{2}E_{\rm ext}^2 \beta V = \frac{1}{4}\eta(\theta_{\rm eff}^E)^2$ removed from the free energy of the system (see the Appendix for further justification of this interpretation using the Hamiltonian formulation). Our normalization $\bar{\mathcal{Z}}_{\rm top}(\eta \to \infty, \theta_{\rm eff}^E) = 1$ corresponds to the geometry when tunneling events are strongly suppressed, i.e., physical phenomena discussed in the present work are trivial for systems in such a limit.

The dual representation for the partition function is obtained by applying the Poisson summation formula such that (24), (26) become

$$\mathcal{Z}_{\rm top}(\eta,\theta^E_{\rm eff})=\frac{1}{\sqrt{\pi\eta}}\sum_{n\in\mathbb{Z}}\exp\left[-\frac{n^2}{\eta}+{\rm i}n\cdot\theta^E_{\rm eff}\right]$$
$$\tilde{\mathcal{Z}}_{\rm top}(\eta,\theta^E_{\rm eff})=\exp\left[\frac{\eta(\theta^E_{\rm eff})^2}{4}\right]\times\mathcal{Z}_{\rm top}(\eta,\theta^E_{\rm eff}). \quad (27)$$

Unfortunately, we cannot directly calculate physically meaningful thermodynamic properties of the system from this partition function, since $\theta^E_{\rm eff}$ does not represent a physical electric field living in Minkowski space-time. Rather, we need to first switch to a Minkowski field by the formal replacement $E_{\rm Euclidean}\to iE_{\rm Minkowski}$. Explicitly, the partition function in the presence of a real Minkowski electric field is given by

$$\tilde{\mathcal{Z}}_{\rm top}(\eta,\theta^M_{\rm eff})=\sum_{k\in\mathbb{Z}}\exp\left[-\eta(\pi^2k^2+i\pi k\theta^M_{\rm eff})\right], \quad (28)$$

where the physical Minkowski electric field $E^{\rm Mink}_{\rm ext}$ enters the partition function $\mathcal{Z}_{\rm top}(\eta,\theta^M_{\rm eff})$ through the combination

$$\theta^M_{\rm eff}=eL_3\beta E^{\rm Mink}_{\rm ext}=-i\theta^E_{\rm eff}. \quad (29)$$

Our interpretation in this case remains the same: in the presence of a physical external electric field $E^{\rm Mink}_{\rm ext}$ represented by the complex source $\theta^E_{\rm eff}$, the path integral (24) is saturated by the Euclidean configurations (12) describing physical tunneling events between the topological sectors $|k\rangle$.

With an external Minkowski electric field, the z-direction topological pressure computed from the partition function (28) exhibits oscillatory behavior with respect to $\theta^M_{\rm eff}$. A notable feature of the pressure is that the oscillation period depends on the dimensionless parameter η characterizing the system (16), in marked contrast to the magnetic case [1], where there is a universal 2π periodicity for all values of τ.

To illustrate the $\theta^M_{\rm eff}$ dependence of the observables, first consider a simple case with $\eta\gg1$, where the magnitude of all effects is exponentially small. In this limiting case for sufficiently small external field $E^{\rm Mink}_{\rm ext}$ one can keep only the lowest branch with $k=\pm1$ in Eq. (28) such that the expression for the pressure assumes the form

$$P_{\rm top}(0\le\eta\pi\theta^M_{\rm eff}\le\pi)\approx\frac{e^2\pi^2\eta^2}{L_1^2L_2^2}\exp(-\pi^2\eta)\left[\cos(\pi\eta\theta^M_{\rm eff})+\frac{(\pi\eta\theta^M_{\rm eff})}{\pi^2\eta}\sin(\pi\eta\theta^M_{\rm eff})\right]. \quad (30)$$

This formula is valid only for the first branch when the electric field is small, $\eta\pi|\theta^M_{\rm eff}|\le\pi$. When the external field becomes stronger one should be more careful with formal differentiation of the partition function (28) with respect to external parameters. This is because the partition function is a periodic function of $\theta^M_{\rm eff}$, and this periodicity must be respected by all physical observables. Using the periodicity, one can always separate out an integer multiple of 2π from stronger fields, $\eta\pi\theta^M_{\rm eff}=2\pi m+[\eta\pi\theta^M_{\rm eff}-2\pi m]$, such that the pressure in the second branch, $\pi\le\eta\pi\theta^M_{\rm eff}\le2\pi$, assumes the form

$$P_{\rm top}(\pi\le\eta\pi\theta^M_{\rm eff}\le2\pi)\approx\frac{e^2\pi^2\eta^2}{L_1^2L_2^2}\exp(-\pi^2\eta)\times\left[\cos(\pi\eta\theta^M_{\rm eff})+\frac{(2\pi-\pi\eta\theta^M_{\rm eff})}{\pi^2\eta}\sin(2\pi-\pi\eta\theta^M_{\rm eff})\right]. \quad (31)$$

Thus, the second term in the square brackets in (30) and (31) explicitly exhibits the cusp singularity at the point $\pi\eta\theta^M_{\rm eff}=\pi$. Such behavior is, in fact, a quite generic feature of gauge systems as a result of twofold degeneracy and level-crossing phenomena, see footnote[2] for more comments and references.

Indeed, the degeneracy can be observed from the partition function (28), which explicitly exhibits the double degeneracy at $\pi\eta\theta^M_{\rm eff}=\pi$ when the level crossing occurs. One can approach the point $\pi\eta\theta^M_{\rm eff}=\pi$ from two sides using a mirrorlike symmetry: $\pi\eta\theta^M_{\rm eff}\to(2\pi-\pi\eta\theta^M_{\rm eff})$. It can be easily checked that this does not modify the partition function itself as the corresponding sign flip in the topological term is equivalent to relabeling $k\to-k$ in the sum $k\in\mathbb{Z}$ in Eq. (28). An analogous phenomenon is known to occur in the 2D Schwinger model, where the system shows twofold degeneracy at $\theta=\pi$. It also occurs in the 4D Maxwell system saturated by the magnetic instantons, as discussed in detail in [2].

Numerically, for a sufficiently small $\eta\sim0.25$, where the effect is expected to be at its maximum, the pressure as a function of $\theta^M_{\rm eff}$ is shown in Fig. 2 and cusp singularities

[2]To be more precise, the physics is periodic under the shift $\pi\eta\theta^M_{\rm eff}\to\pi\eta\theta^M_{\rm eff}+2\pi m$. Similar periodicity with respect to an external parameter is quite generic in many gauge theories, including QCD, where all physical observables are periodic functions of the fundamental θ parameter. This periodicity can be formally enforced in our case in the path integral by replacing $\pi\eta\theta^M_{\rm eff}\to\pi\eta\theta^M_{\rm eff}+2\pi m$ in Eq. (28) and summing over $m\in\mathbb{Z}$. This is in fact a conventional procedure in similar systems, see, e.g., Eq. (52) in [15], where theoretically controllable computations have been performed in a weakly coupled non-Abelian gauge theory. A generic consequence of this periodicity is that the system shows cusp singularities at specific points, normally $\theta=\pi+2\pi m$. The origin for such behavior is the twofold degeneracy emerging in the system at these points. As a result of this degeneracy, level crossing occurs precisely at these points when the branch with the minimum free energy (corresponding to the ground state) changes, see [15] for a large number of references to the original literature.

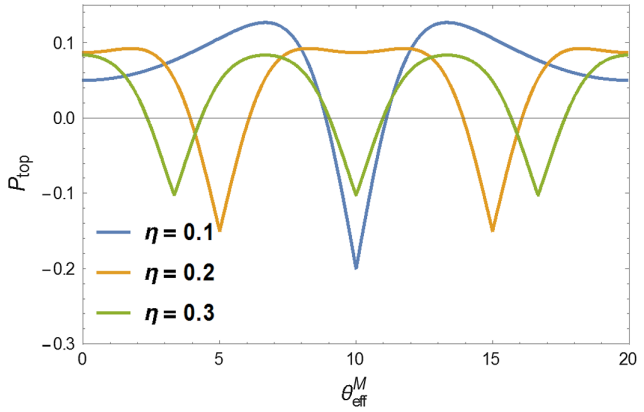

FIG. 2. The topological Casimir pressure plotted in units of $e^2/2L_1^2L_2^2$. There is a clear dependence of oscillation periodicity on η, in sharp contrast to the universal 2π periodicity in the topological pressure in the magnetic system [1]. To make the pressure strictly periodic, Eq. (19) is used in the first branch, $|\pi\eta\theta^M_{\rm eff}| < \pi$, and the results are then repeated over subsequent branches, see text for details.

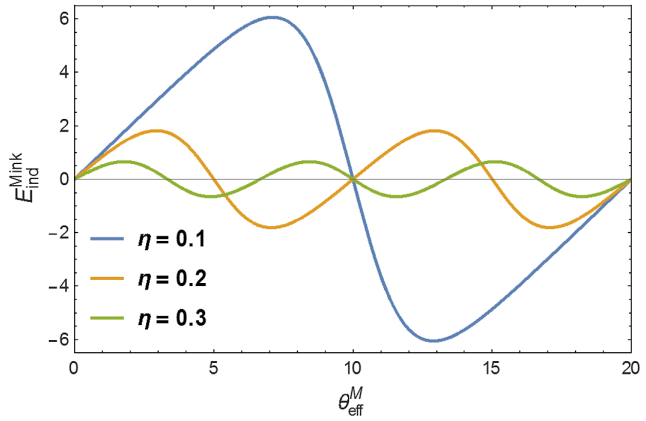

FIG. 3. The induced electric field in units of $1/e\beta L_3$ in the presence of an external electric field in Minkowski space-time. The oscillation period and amplitude increase for smaller η's. The same plot also serves as the induced dipole moment measured in units $\frac{L_1L_2L_3}{e\beta L_3} = \frac{e}{2}L_3\eta$, see Secs. V, VI for the details.

emerge at $\pi\eta\theta^M_{\rm eff} = \pi + 2\pi m$. One can explicitly see that the system is symmetric under $\pi\eta\theta^M_{\rm eff} \to 2\pi - \pi\eta\theta^M_{\rm eff}$, and it also exhibits the periodicity $\pi\eta\theta^M_{\rm eff} \to \pi\eta\theta^M_{\rm eff} + 2\pi m$, as expected.

One can also compute the induced electric field in response to the external source $\theta^M_{\rm eff}$ in Minkowski space by differentiating the partition function $\bar{\mathcal{Z}}_{\rm top}(\eta, \theta^M_{\rm eff})$ with respect to $E^{\rm Mink}_{\rm ext}$:

$$\langle E^{\rm Mink}_{\rm ind}\rangle = -\frac{1}{\beta V}\frac{\partial \ln \bar{\mathcal{Z}}_{\rm top}}{\partial E^{\rm Mink}_{\rm ext}} = -\frac{e}{L_1L_2}\frac{\partial \ln \bar{\mathcal{Z}}_{\rm top}}{\partial \theta^M_{\rm eff}} = \frac{1}{\bar{\mathcal{Z}}_{\rm top}}\sum_{k\in\mathbb{Z}}\frac{2\pi k}{eL_3\beta}e^{-\eta\pi^2k^2}\sin[\pi k\eta\theta^M_{\rm eff}], \tag{32}$$

plotted in Fig. 3.

It is quite obvious that $\langle E^{\rm Mink}_{\rm ind}\rangle = 0$ if $E^{\rm Mink}_{\rm ext} = 0$. The difference in comparison to the analogous expression from [1] is that our present definition of the induced field does not include the external piece $E^{\rm Mink}_{\rm ext}$, in contrast to the definition used in [1], where the induced field of the system was defined as the total field (i.e., the truly induced field plus the external piece). One can observe that the induced field $\langle E^{\rm Mink}_{\rm ind}\rangle$ changes the sign under the mirrorlike symmetry $\pi\eta\theta^M_{\rm eff} \to 2\pi - \pi\eta\theta^M_{\rm eff}$ in contrast to the expression for the pressure presented in Fig. 2. This is because the induced field $\sim\partial/\partial\theta^M_{\rm eff}$ flips the sign under this symmetry, in contrast with the pressure $P_{\rm top} \sim \partial/\partial L_3$.

A few comments are in order. First, formula (32) represents the physical induced field defined in Minkowski space-time. In addition, the oscillations now occur with periodicity $\pi\eta\theta^M_{\rm eff} = 2\pi m$, which can be identically rewritten as

$$\pi\eta\theta^M_{\rm eff} = 2\pi m \Rightarrow L_1L_2E^{\rm Mink}_{\rm ext} = em. \tag{33}$$

Note that this value for the physical electric field is indeed consistent with the results from the canonical Hamiltonian approach in the Appendix. It further supports our formal manipulations in the transition from the Euclidean to the Minkowski description.

We should emphasize that the quantization $L_1L_2E^{\rm Mink}_{\rm ext} = em$ of the physical electric field (33) is drastically different than the quantization of the Euclidean instanton fluxes (12) saturating the partition function. Indeed, the instanton fluxes have a different normalization factor $e \to \frac{2\pi}{e}$ along with the geometric factor $L_1L_2 \to L_3\beta$. It should be contrasted with the magnetic case [1], where the external field and the instanton fluxes have the same periodic properties. This is precisely the reason why formulas from [1] exhibit the universal periodic properties, in contrast to (32).

In the large η limit one can again keep only two terms in Eq. (32) with $k = \pm 1$, such that it assumes the following simple form:

$$\langle E^{\rm Mink}_{\rm ind}\rangle = \frac{4\pi e^{-\eta\pi^2}}{eL_3\beta}\sin(\pi\eta\theta^M_{\rm eff}). \tag{34}$$

As expected, the induced term has nonanalytical $\exp(-1/e^2)$ behavior and cannot be seen in perturbation theories, as it originates from the tunneling events. It is exponentially suppressed when $\eta \to \infty$ as expected, and obviously vanishes in the $\theta^M_{\rm eff} \to 0$ limit.

Similarly, we can compute the (topological) susceptibility of the system, which measures the response of free energy to the introduction of a source term, represented by $E^{\rm Mink}_{\rm ext} \sim \theta^M_{\rm eff}$ in our case:

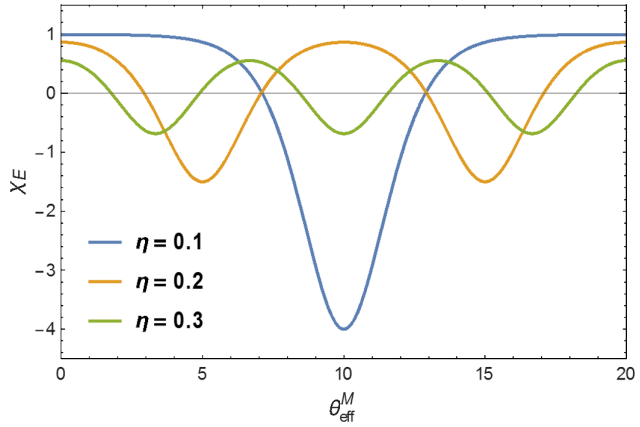

FIG. 4. The electric susceptibility of the system in response to different values of the external electric field. It is nonvanishing even at $\theta^M_{\rm eff} = 0$ due to topological fluctuations. The oscillations have η-dependent periodicity: $2/\eta$.

$$\chi_E = -\frac{2}{\eta}\frac{\partial^2}{\partial {\theta^M_{\rm eff}}^2} \ln \bar{\mathcal{Z}}_{\rm top}(\eta, \theta^M_{\rm eff}), \tag{35}$$

shown in Fig. 4.

In the large η limit, one can explicitly check using the analytical expression (28) that $\chi_E \sim \exp[-\eta\pi^2]$ is strongly suppressed, consistent with our expectation that no electric correlations exist in the conventional Casimir effect setup. The χ_E is symmetric under the mirrorlike symmetry $\pi\eta\theta^M_{\rm eff} \to 2\pi - \pi\eta\theta^M_{\rm eff}$, as the second derivative $\partial^2/\partial {\theta^M_{\rm eff}}^2$ does not flip the sign at the degeneracy point $\pi\eta\theta^M_{\rm eff} = \pi$.

V. INDUCED DIPOLE MOMENT AND SURFACE CHARGES

Although the electric instanton fluxes describing the tunneling events between topological sectors in our system are formulated in Euclidean space-time (12), we have shown in the previous section that a real-valued electric field will be induced in Minkowski space-time in response to a nonvanishing $\theta^{\rm M}_{\rm eff}$. In this section, we represent this induced electric field in the bulk of the system in terms of the surface effects. In other words, we want to reformulate the fluctuations of the topological electric fluxes using fluctuating surface charges on the plates.

A similar reformulation of the problem was carried out for the magnetic case in [4], where it was explicitly shown that the tunneling instanton effects can be understood in terms of fluctuating topological nondissipating currents, which unavoidably will be generated on the boundaries. In [4], the system was a cylinder with radius R and height L_3 with the topological current J^ϕ flowing in the ϕ direction on its infinitely thin boundary. It has also been noted that these topological currents are very similar in nature, but not the same as the well-known persistent currents normally observed on metallic (not superconducting) rings, see references on the original experimental and theoretical studies on persistent currents in [4]. In all cases the effects are due to the coherent Aharonov-Bohm phases correlated over macroscopically large distances, although the nature of the long-range coherence is different for our topological nondissipating currents and for the well-known persistent currents.

The duality between magnetic and electric fields in the Maxwell system strongly suggests that similar topological effects must be present in the electric systems as well. Essentially we attempt to study the effects which are electromagnetically (EM) dual to the persistent currents observed on metallic rings. The relevant formal construction indeed can be easily carried out, as we have shown in Secs. III and IV.

We start with an explicit demonstration that the existence of an induced electric field (generated by the electric instantons) in Minkowski space (32) suggests that one can effectively recast the mathematics into an equivalent form where physical electric charges are induced on each plate of the capacitor.[3] These charges have pure quantum origin and are, in all respects, very similar to the persistent nondissipating currents induced by the magnetic instantons discussed in [4].

An important technical comment here is that the induced electric field (32) can be thought of as the polarization of the system per unit volume, i.e., $\langle P\rangle = -\langle E^{\rm Mink}_{\rm ind}\rangle$, since the definition for $\langle P\rangle$ is identical to (32) up to a minus sign because it enters the Hamiltonian as $H = -\vec{P}\cdot\vec{E}_{\rm ext}$. Therefore, we arrive at the following expression for the induced electric dipole moment of the system in the presence of an external electric field $E^z_{\rm ext}$,

$$\begin{aligned}\langle p^{\rm Mink}_{\rm ind}\rangle &= -\langle E^{\rm Mink}_{\rm ind}\rangle L_1L_2L_3 \\ &= -\frac{1}{\bar{\mathcal{Z}}_{\rm top}}\sum_{k\in\mathbb{Z}}\frac{2\pi k L_1L_2}{e\beta}\, e^{-\eta\pi^2k^2}\sin(\pi k\eta\theta^M_{\rm eff}).\end{aligned} \tag{36}$$

Based on this interpretation, one can view Fig. 3 as a plot for the induced electric dipole moment in units of $\frac{1}{2}\eta e L_3$, which represents the correct dimensionality e · cm for the electric dipole moment.

One can understand the same formula (36) using the original expression for the coupling between the external field and the topological instantons,

$$\int {\rm d}^4x(\vec{E}_{\rm ext}\cdot\vec{E}_{\rm top}) = \int {\rm d}^4x V_{\rm ext}(\vec{\nabla}\cdot\vec{E}_{\rm top}), \tag{37}$$

where we have neglected a total divergence term. The cross term written in the form (37) strongly suggests that

[3]We briefly remark that the charges indeed physically reside on the actual plates as long as the periodic boundary conditions are enforced using the quantum LC circuit configuration.

$(\vec{\nabla}\cdot\vec{E}_{\rm top})$ can be interpreted as surface charges generated on the plates. Indeed, if we use Eq. (12) for the topological instantons $\vec{E}_{\rm top}$ describing the tunneling transition to the $|k\rangle$ sector, we arrive at the following formula for the surface charge density:

$$\sigma^{\rm Mink}_{\rm ind}(k)=\frac{2\pi k}{e\beta L_3}[\delta(x_3)-\delta(x_3-L_3)]. \tag{38}$$

This formula implies that an electric dipole moment will be generated in each topological sector $|k\rangle$, given by

$$p^{\rm Mink}_{\rm ind}(k)=-\frac{2\pi L_1L_2}{e\beta}k, \tag{39}$$

which reproduces the relevant term in (36), derived in a quite different way without any mention of surface charges.

Furthermore, one can explicitly check that the cross term (37) expressed in terms of the surface charge $\sigma^{\rm Mink}_{\rm ind}(k)$ exactly reproduces the corresponding term in the action of the partition function (28) computed in terms of the bulk instantons. Indeed, the cross term in the action is

$$\begin{aligned}\int {\rm d}^4x(\vec{E}_{\rm ext}\cdot\vec{E}_{\rm top})&=\int {\rm d}^4xV_{\rm ext}(\vec{\nabla}\cdot\vec{E}_{\rm top})\\&=\int {\rm d}^4x(E_{\rm ext}x_3)\left(\frac{2\pi k}{e\beta L_3}\right)\delta(x_3-L_3)\\&=\pi\eta k\theta^E_{\rm eff},\end{aligned} \tag{40}$$

where we have substituted $V_{\rm ext}=-x_3E_{\rm ext}$ and expressed the external field in terms of $\theta^E_{\rm eff}$. Equation (40) precisely coincides with the cross term $\sim k$ in the action $\exp(-S)$ for the partition function (26). In the same way the classical instanton action $\sim k^2$ in (26) can be also understood in terms of the surface charges.

The basic point of our discussions in this section is that the expression for the induced electric dipole moment (36) can be understood in terms of an induced field, according to (32). The same effect can be also interpreted in terms of the surface charges of the system as (38) and (39) suggest. However, the origin of the phenomena is not these charges but the presence of the topological $|k\rangle$ sectors in Maxwell $U(1)$ electrodynamics formulated on a compact manifold with nontrivial mappings $\pi_1[U(1)]=\mathbb{Z}$. Such $|k\rangle$ sectors exist and transitions between them always occur, even if charged particles are not present in the bulk of the system. The secondary role played by the charged particles is in particular illustrated by the fact that the extra contribution to the Casimir vacuum pressure generated by $\bar{\mathcal{Z}}_{\rm top}$ survives a vanishing external field, but the fluctuating positive and negative charges cancel each other exactly. The fundamental explanation is still the tunneling transitions between vacuum winding states which occur regardless of the value of the external field.

To conclude this section, we would like to remark that it is quite typical in condensed matter physics that topologically ordered systems allow such a complementary formulation in terms of the physics on the boundary. Therefore, it is not a surprise that we can reformulate the original instanton fluctuations saturating $\bar{\mathcal{Z}}_{\rm top}(\eta,\theta^E_{\rm eff})$ in terms of the boundary surface charges which always accompany these instanton transitions. See more discussions on the relation between descriptions in the bulk and on the surface for the magnetic system in [4].

VI. NUMERICAL ESTIMATES FOR A QUANTUM LC CIRCUIT

Our goal now is to discuss a possible design where such electric effects can be (at least in principle) studied. In what follows we consider a two-plate capacitor with area L_1L_2 separated by distance $L_3\ll L_1,L_2$ at temperature β^{-1}. The two plates are connected by an external wire such that charges can freely move from one plate to the other. The system can be viewed as a quantum LC circuit where conventional quantum transitions (due to ordinary degrees of freedom) are replaced by tunneling transitions as described in the previous sections. The vacuum between the plates (where these tunneling transitions occur) represents the object of our studies.

We would like to make a few numerical estimates for illustrative purposes only. The first set of parameters is motivated by the accurate measurement of the CE using parallel plates [16] (see also [17], where historically the first accurate measurement was performed, but for a different geometry). The second set of parameters is motivated by the experiments on persistent currents [18] where the correlation of the Aharonov-Bohm phases is known to be maintained. While the persistent current is a magnetic phenomenon, the EM duality strongly suggests that a similar electric effect should also occur when the coherent Aharonov-Bohm phases are correlated on macroscopically large distances. Therefore, for the second set of parameters we adopt the typical sizes of the magnetic system (where persistent currents have been observed) to estimate the topological effects for our electric capacitor. Before we proceed to the numerical estimates, it is worthwhile to compare and contrast the conventional persistent current and the topological current, and explain the rationale behind using the second set of estimation parameters.

A. Persistent currents and Aharonov-Bohm phases

The mesoscopic phenomenon of persistent currents occurs in resistive metal rings at low temperatures [18,19]. The electron waves in the metal undergo interference and exhibit sensitivity to external magnetic fields. Without any magnetic field, the electrons fluctuate symmetrically between clockwise and counterclockwise directions and give rise to a vanishing total current. At nonzero

magnetic fields, persistent currents are often formulated in terms of an Aharonov-Bohm flux ϕ threading the ring: electrons coupled to the gauge field pick up Aharonov-Bohm phases as they move clockwise and counterclockwise in the ring, and their interference gives rise to a periodically varying electric current with periodicity $\phi_0 = h/e$. Note that the persistent current is an equilibrium phenomenon, i.e., no supply of power is needed to maintain this current, hence its name.

A number of realistic constraints can affect the magnitude of the observed current: the temperature of the system must be low enough so that thermal fluctuations do not disturb the coherence of the electron wave functions over the relevant length scales; and the scattering of the electrons by impurities, defects, and imperfect surfaces of the material also serves to reduce the mean free path of the electrons. In order for sizable currents to be observed, the electrons must be coherent over a length scale comparable to the circumference of the metal ring in order to experience Aharonov-Bohm type interference. Therefore, experiments are usually performed on rings with a circumference of a few micrometers at temperatures below 500 mK.

For the magnetic system reviewed in Sec. II, an external magnetic field induces a magnetic dipole moment, which has been equivalently formulated in terms of a topological nondissipating current flowing along the boundary [4]. Although the topological current is similar in nature to the observed persistent current, it is nevertheless not identically the same and represents an independent additional contribution to the conventional persistent current. In the conventional case, Aharonov-Bohm coherence is determined by the dynamics of the electrons residing on the ring, while in our case it is determined by the dynamics of the vacuum, i.e., tunneling transitions between the vacuum winding sectors. This difference, in particular, manifests itself in the properties of the induced magnetic moment: it is quantized in our case, while it can assume any value for conventional persistent currents.

Indeed, one can easily compute the induced dipole moment by differentiating $\mathcal{Z}_{\rm top}$ from Eq. (9) with respect to the external magnetic field. The result is [4]

$$\langle m^z_{\rm ind}\rangle = \frac{1}{\beta}\frac{\partial \ln \mathcal{Z}_{\rm top}}{\partial B^{\rm ext}_z} = -\langle B_{\rm ind}\rangle L_3 \pi R^2 = -\frac{L_3 2\pi}{e}\frac{\sqrt{\tau\pi}}{\mathcal{Z}_{\rm top}}\sum_{k\in\mathbb{Z}}\left(\frac{\theta_{\rm eff}}{2\pi}+k\right)\exp\left[-\tau\pi^2\left(k+\frac{\theta_{\rm eff}}{2\pi}\right)^2\right]. \tag{41}$$

The first term in the round brackets can be identified with the external background field, while the term proportional to k assumes the form

$$m^z_{\rm ind}(k) = -\frac{2\pi L_3}{e}k, \tag{42}$$

and can be interpreted as the magnetic moment in the $|k\rangle$ sector. The important observation here is that the induced magnetic moment per unit length $m^z_{\rm ind}(k)/L_3$ is quantized. This property should be contrasted with conventional persistent currents for which the magnetic moment per unit length can assume any value. This shows once again that the persistent currents and topological currents are very similar in nature, but still they originate from different physics.

In addition, the two types of currents behave very differently when external parameters, such as sizes, vary. Indeed, numerical estimates performed on a realistic metal ring system [4] suggest that if the ideal boundary conditions required for the TCE could be satisfied while keeping the dimensionless parameter $\tau \sim 1$, then the magnitude of the topological current is at least 3 orders of magnitude larger than the persistent current reported in [18]. At the same time, if one uses exactly the same parameters of the sample in [18], then the corresponding topological current would produce a contribution many orders of magnitude smaller than the observed persistent current.

Although the conventional persistent currents and the topological currents are different phenomena, they both rely on the electron wave functions being coherent over a length scale comparable to the system dimension in a pure gauge configuration. Based on EM duality, one could argue that if Aharonov-Bohm coherence has been established for the magnetic system, it is likely to hold in electric systems with similar geometric sizes as well. And this forms the rationale for our second set of parameters in the following analysis.

B. Numerical estimates

First, we adopt the system sizes from the first accurate measurement of the Casimir effect using parallel plates [16]. Unlike the magnetic system studied in [1], the dimensions of this electric system as represented by η can be fairly easily optimized to maximize the topological effect. In this experiment a small capacitor was formed using chromium-coated surfaces with area $L_1 L_2 = 1.2 \times 1.2$ mm^2 and separation L_3 in the $0.5 - 3$ μm range. This geometry corresponds to $\eta \gg 1$ and for reasons explained previously, we expect the topological effect to be vanishingly small. However, if plate separation could be increased to 0.4 mm (such that our approximation $L_3 \ll L_1, L_2$ is still marginally satisfied) and the ambient temperature set to 10 mK (corresponding to $\beta = 180$ mm), then

$$\eta^{(I)} = \frac{2L_1 L_2}{e^2 \beta L_3} = \frac{1.2 \times 1.2 \text{ mm}^2}{2\pi\alpha(180 \text{ mm})(0.4 \text{ mm})} \approx 0.4, \tag{43}$$

where the intensity of the topological tunneling transitions assumes the maximum values, see Fig. 1. The effect is still much smaller than the conventional Casimir effect, as we already discussed in Sec. III B. The main point, however, is

that the effect is highly sensitive to the external field, in contrast to the conventional CE, as argued in Sec. IV. Precisely this sensitivity might be the key element for observing this fundamentally novel phenomenon when the vacuum energy in the bulk is not associated with any physical degrees of freedom propagating in the bulk.

Now we want to consider a second set of parameters motivated by observing the persistent currents. The connection between the conventional persistent current and the topological current has been explained in Sec. VI A. Therefore, we expect the topological tunneling transitions to be present in the system when the ring area πR^2 in the magnetic system [18] is replaced by the electric capacitor plate area L_1L_2, and the ring width replaced by the plate separation L_3. With this correspondence, we estimate the key dimensionless parameter η to be

$$\eta^{(II)} = \frac{2L_1L_2}{e^2\beta L_3} = \frac{2\pi(1.2\mu m)^2}{4\pi\alpha(0.6\text{ cm})(0.1\mu\text{m})} \approx 0.16, \qquad (44)$$

where we have used $L_3 \sim 0.1$ μm and $\beta \sim 0.6$ cm corresponding to the temperature $T \simeq 300$ mK below which the electron phase coherence length is sufficiently large and temperature independent.[4] This parameter falls into the region where the intensity of the topological tunneling transitions assumes its maximum values, see Fig. 1. Therefore, one should anticipate a nonzero value for the induced electric dipole moment when an external field is applied.

Assuming appropriate boundary conditions (i.e., periodic up to a large gauge transformation) are established, the induced electric dipole moment depends on the applied external field. The corresponding dependence of $\langle p^{\text{Mink}}_{\text{ind}}\rangle$ on the external field can be easily established from Fig. 3, where the plot should be understood as the induced dipole moment in units of $E_{\text{ind}}L_1L_2L_3 = \frac{eL_3}{2}\eta$. Numerically, these units for our two sets of parameters can be estimated as

$$\langle p^{\text{Mink}}_{\text{ind}}\rangle^{(I)} \approx \frac{eL_3}{2}\eta^{(I)} \sim 0.1(e\cdot\text{mm})$$
$$\langle p^{\text{Mink}}_{\text{ind}}\rangle^{(II)} \approx \frac{eL_3}{2}\eta^{(II)} \sim 0.01(e\cdot\mu\text{m}). \qquad (45)$$

The numerical estimates for the induced dipole moment due to the coherent tunneling effects (45) do not look very promising if measurements are performed with a static external electric field. In the next section we consider a possibility when the external field varies with time. In this case one should anticipate the emission of real propagating photons which leave the system, and which hopefully (in principle) can be detected.

[4]One should remark here that there are related effects when the entire system can maintain coherent Aharonov-Bohm phases at very high temperatures $T \simeq 79$ K [20].

VII. ELECTRODYNAMICS AND E&M RADIATION

Up till this point, we have implicitly assumed that the external electric field $E^{\text{Mink}}_{\text{ext}}$ is static. However, Eq. (36) still holds in the case of a dynamical external field $E^{\text{Mink}}_{\text{ext}}(t)$ as long as its time dependence is adiabatically slow compared to all relevant time scales of the system. Then this time dependence simply enters the partition function through $\theta^M_{\text{eff}}(t)$. In has been argued in [4] that as the induced magnetic dipole moment varies in response to an adiabatically oscillating external source, real photons will be emitted through magnetic dipole radiation. Following the same reasoning, we can also compute the electric dipole radiation produced by our capacitor.

Therefore, one can use the well-known expressions for the intensity $\vec{S}$ and total radiated power I for the electric dipole radiation when the dipole moment (36) varies with time:

$$\vec{S} = I(t)\frac{\sin^2\theta}{4\pi r^2}\vec{n}, \qquad I(t) = \frac{2}{3c^2}\langle \ddot{p}^{\text{Mink}}_{\text{ind}}(t)\rangle^2. \qquad (46)$$

In the case where the external electric field plotted in Fig. 3 is almost linear, the approximate induced dipole moment, $E^z_{\text{ext}}(t)$, varies linearly, as one can see from Fig. 3. In particular, if $E^z_{\text{ext}}(t) \sim \cos\omega t$, then $\langle \ddot{p}^{\text{Mink}}_{\text{ind}}\rangle \sim \omega^2\cos\omega t$. In this case one can easily compute the average intensity over a large number of completed cycles with the result

$$\langle I\rangle \sim \frac{\omega^4}{3c^2}\langle p^{\text{Mink}}_{\text{ind}}\rangle^2, \qquad (47)$$

where $\langle p^{\text{Mink}}_{\text{ind}}\rangle$ is given by (36).

This electromagnetic radiation has a simple explanation in terms of the fluctuating charges that reside on the capacitor plates (38). For static external field $E^{\text{Mink}}_{\text{ext}}$, the charge density on each plate also stays constant, giving rise to a time-independent electric dipole moment. But when $E^{\text{Mink}}_{\text{ext}}(t)$ starts to fluctuate, the induced dipole moment also acquires time dependence, naturally leading to the emission of real photons.

The detection of this radiation could be made easier by taking advantage of the system's twofold degeneracy at $\theta^M_{\text{eff}} \in \{1/\eta + 2n/\eta : n \in \mathbb{Z}\}$, corresponding to half integer fluxes, where the system's ground state reconstructs itself [2]. As the external field slowly sweeps through these points, $\langle p^{\text{Mink}}_{\text{ind}}\rangle$ quickly changes polarity, as Fig. 3 shows, producing high amounts of radiation. This will hopefully set the topological emission apart from the uninteresting radiation due to the fluctuating external source. In addition, since the power radiated electrically usually substantially exceeds that radiated magnetically for systems with comparable dimensions, we expect the radiation from this present electric configuration to be much more readily detectable than the one in [4].

VIII. CONCLUSION AND SPECULATIONS

In this work we have discussed a number of very unusual features exhibited by the Maxwell theory formulated on a compact manifold $\mathbb{M}$ with nontrivial topological mappings $\pi_1[U(1)]$, which was termed the topological vacuum ($\mathcal{TV}$). All these features originate from the topological portion of the partition function $\mathcal{Z}_{\rm top}$, which cannot be described by a construction of conventional photons expanded near a classical vacuum $|n\rangle$. In other words, all effects discussed in this paper have a nondispersive nature.

The computations of the present work along with previous calculations in [1–4] imply that the extra energy, not associated with any physical propagating degrees of freedom, may emerge in a gauge system if some conditions are met. This fundamentally new type of energy emerges as a result of the dynamics of pure gauge configurations.

The new idea advocated in this work is that this new type of energy might be related to electric-type instantons, in contrast with the magnetic-type instantons studied in the previous papers. While the modification may look minor, it leads to a number of novel effects. Most notably, whereas the magnetic oscillations have universal 2π periodicity for all system sizes, the periodicity in the electric system varies with the system size. It remains to be seen if the effects discussed in the present work can be experimentally observed.

In addition, the electric system studied in the present work could be considered as a simple toy model where the topological tunneling transitions can be theoretically studied. These novel effects could have some profound consequences for astrophysics and cosmology if they persist in the Standard Model (SM). Indeed, the concept of gauge symmetry is central to the SM. As a result, the existence of such nontrivial homotopy mappings implies that the ground state of the system should be represented by a superposition of the topological winding sectors. The corresponding path integral which determines the system therefore must also include the sum over all the topological sectors, accounting for the physics describing the tunneling transitions between them.

All the effects studied in Secs. III and IV were precisely attributed to the physics of tunneling transitions which generate an additional vacuum energy. The effects are obviously nonlocal in nature. Moreover, the corresponding contributions to the correlation functions are represented by nondispersive terms which fundamentally cannot be expressed in terms of any local propagating degrees of freedom. Furthermore, the radiation of real physical photons described in Sec. VII represents a fundamentally novel mechanism of particle production (*à la* the dynamical Casimir effect) when the emission occurs from the topological vacuum due to the tunneling transitions, rather than from the decay of some local propagating degrees of freedom.

We note that many conventional approaches to describe the dark vacuum energy (or vacuum inflation) are based on effective local field theories. The production of real particles (during the so-called reheating epoch) is also normally considered as a result of the conventional local interaction of real particles.

The unique features of the system studied in the present work when an extra energy is not related to any physical propagating degrees of freedom was the main motivation for a proposal [21,22] that the vacuum energy of the Universe may have, in fact, precisely such a nondispersive and nonlocal nature[5] studied in the present work in a toy model. This proposal where an extra energy cannot be associated with any propagating particles should be contrasted with the conventional description where an extra vacuum energy in the Universe is always associated with some *ad hoc* physical propagating degrees of freedom, such as inflaton.[6]

ACKNOWLEDGMENTS

This research was supported in part by the Natural Sciences and Engineering Research Council of Canada. C. C. was supported in part by the Walter Burke Institute for Theoretical Physics at Caltech, U.S. DOE Grant No. DE-SC0011632, and the Gordon and Betty Moore Foundation through Grant No. 776 to the Caltech Moore Center for Theoretical Cosmology and Physics. Y. Y. acknowledges a research award from the UBC Work Learn Program.

APPENDIX: HAMILTONIAN APPROACH

We check the topological partition function with an external electric field using canonical quantization so there is no ambiguity regarding the physical meaning of the electric field. Recall the classical Lagrangian density for the EM field

$$\mathcal{L}(x) = \frac{1}{2}(\mathbf{E}^2 - \mathbf{B}^2), \tag{A1}$$

where $E_i = -\partial_i A_0 + \partial_0 A_i$ and $B_i = -\epsilon_{ijk}\partial_j A_k$. We then proceed with the usual Hamiltonian formalism where we

[5]This new type of vacuum energy which cannot be expressed in terms of propagating degrees of freedom is well known to the QCD community and has been well studied in QCD lattice simulations, see [21,22] for references and details.

[6]There are two instances in the evolution of the Universe when the vacuum energy plays a crucial role. The first instance is identified with the inflationary epoch when the Hubble constant H was almost constant, which corresponds to the de Sitter–type behavior $a(t) \sim \exp(Ht)$, with exponential growth of the size $a(t)$ of the Universe. The second instance when the vacuum energy plays a dominant role corresponds to the present epoch when the vacuum energy is identified with the so-called dark energy $\rho_{\rm DE}$, which constitutes almost 70% of the critical density. In the proposal [21,22] the vacuum energy density can be estimated as $\rho_{\rm DE} \sim H\Lambda_{\rm QCD}^3 \sim (10^{-4}\ {\rm eV})^4$, which is amazingly close to the observed value.

realize that A_0 is nondynamical and imposes the Gauss's law constraint as a Lagrange multiplier. Hence the Hamiltonian density is given by

$$\mathcal{H}(x) = \frac{1}{2}(\mathbf{E}^2 + \mathbf{B}^2) - A_0(x)\nabla \cdot \mathbf{E}(x). \tag{A2}$$

We can fix the $A_0 = 0$ gauge and define the Hamiltonian $H = \int d^3x \mathcal{H}(x)$.

Then, we follow the usual quantization procedure for the EM field by imposing the equal time commutation relations

$$[\hat{A}_j(\mathbf{x}), \hat{\Pi}_k(\mathbf{y})] = i\delta(\mathbf{x} - \mathbf{y})\delta_{jk}. \tag{A3}$$

The conjugate momentum $\hat{\Pi}_i(x) = -\hat{E}_i$ and potential $\hat{A}_i$ are now promoted to operators, and

$$\hat{E}_j = i\frac{\delta}{\delta A_j(x)}. \tag{A4}$$

We also note the potentials related by a local time-independent gauge transformation are physically equivalent. Namely, $[\hat{Q}(\mathbf{x}), \hat{H}] = 0$, where $\hat{Q}(\mathbf{x}) = \nabla \cdot \mathbf{E}(\mathbf{x})$ generates local time-independent gauge transformations. Consequently, we restrict physical states to the set of gauge invariant subspace of the original Hilbert space and $\hat{Q}(\mathbf{x})|\text{phys}\rangle = 0$. Note that so far we have not imposed any nontrivial boundary conditions.

Now we impose the nontrivial S^1 topology by requiring periodicity in the L_3 direction. Then, in addition to the original small gauge redundancy, we now also have large gauge transformations in the form of

$$A_3 \to A_3 + 2\pi n/eL_3. \tag{A5}$$

Unfortunately, the requirement on only small gauge transformations $[\hat{Q}(x), \hat{H}] = 0$ is no longer sufficient for overall gauge fixing.

This means that the "physical states" from the previous construction with trivial topology now have to be grouped into sectors. We put quotes because they are not really physical anymore as in the previous case. So instead of using a universal label $|\text{phys}\rangle$ for the set of physical states, let us label each set according to their respective sectors, namely, $|\text{phys}_n\rangle$ for the nth sector. In particular, we can see that for each sector, such physical states indeed satisfy $\hat{Q(\mathbf{x})}|\text{phys}_n\rangle = 0$, but under large gauge transformation, we have $\mathcal{T}^{(k)}|\text{phys}_n\rangle = |\text{phys}_{n+k}\rangle$. The large gauge transformation operator $\mathcal{T}^{(k)}$ commutes with the Hamiltonian $[\mathcal{T}^{(k)}, \hat{H}] = 0$. Therefore any physical observables computed without taking into account the sectors are not strictly correct. Furthermore, one has to be careful in not fixing this gauge but sum over all the inequivalent topological n sectors, as they do give rise to physically measurable effects.

As such, one needs to further modify our definition of the physical states (and/or associated Hilbert space). For clarity, we denote the "vacuum" state of each sector by $|n\rangle$ and define $|\theta\rangle = \sum \exp(i\theta n)|n\rangle$ as the new set of physical states which are indeed invariant under all large gauge transformations. The vacuum expectation for a physical observable is then given by $\langle\theta'|\hat{A}|\theta\rangle = \delta(\theta' - \theta)\langle\theta|\hat{A}|\theta\rangle$. It is clear that different values of θ now label the superselection sectors of the theory.

Now we can compute the correct vacuum to vacuum transition (dropping the delta function) from $t = 0$ to $t = t_f$. The Hamiltonian is time independent, thus we get $\langle\theta|e^{-i\hat{H}t_f}|\theta\rangle$. This, as we all know, is the same as performing a related Feynman path integral. The Hamiltonian operator is given by

$$\hat{H} = \int d^3x \frac{1}{2}\left(-\sum_i \frac{\delta^2}{\delta A_i^2} + \mathbf{B}^2\right) \tag{A6}$$

and the partition function is therefore

$$\mathcal{Z} = \text{Tr}(e^{-\beta\hat{H}}). \tag{A7}$$

In 2D it is clear how to proceed as one can solve for the wave functional of A. The 4D computation requires more work due to the physically propagating degrees of freedom.

Nevertheless, we can check the calculation for external electric fields. Adding a physical electric field in the Hamiltonian is straightforward by letting

$$\hat{E}_3 = i\frac{\delta}{\delta A_3} \to i\frac{\delta}{\delta A_3} + E^{\text{M}}_{\text{ext}}, \tag{A8}$$

where $E^{\text{M}}_{\text{ext}}$ is a physical classical electric field (times identity operator) in the z direction. If we diagonalize the matrix according to its appropriate energy eigenfunction(al)s, then

$$\begin{aligned}\mathcal{Z} &= \exp\left(-\frac{1}{2}\beta V(E^{\text{M}}_{\text{ext}})^2\right) \times \text{Tr}\exp(-\beta\hat{H}_{\text{sys}}) \\ &= \mathcal{Z}_{\text{ext}} \times \mathcal{Z}_{\text{sys}},\end{aligned} \tag{A9}$$

where the first factor is nothing but the Boltzmann factor due to the external (applied) electric field in the system, and the Hamiltonian operator inside the trace now assumes the form

$$\hat{H}_{\text{sys}} = \int d^3x \frac{1}{2}\left(-\sum_i \frac{\delta^2}{\delta A_i^2} + \mathbf{B}^2 + 2iE^{\text{M}}_{\text{ext}}\frac{\delta}{\delta A_3} + \ldots\right). \tag{A10}$$

Note that we can factor out this external part, because it does not depend on the quantum fluctuations or the topological sectors. As $\mathcal{Z}_{\text{ext}}$ is not relevant to our discussion, it suffices to preserve the second factor, $\mathcal{Z}_{\text{sys}}$, for analysis of the system.

In particular, we recognize the usual trick and evaluate the quantum partition function using a Euclidean path integral. We obtain the Lagrangian in the usual way and then perform a Wick rotation:

$$\mathcal{Z}_{\rm sys} = \mathcal{Z}_{\rm top} \times \mathcal{Z}_{\rm quant} \tag{A11}$$

$$= \sum_{k\in\mathbb{Z}} \int \mathcal{D}A^{(k)} \exp\left(-\int_0^\beta d\tau \int d^3x \mathcal{L}_E[A^{(k)}]\right), \tag{A12}$$

where $A^{(k)}$ is understood to be periodic in β, k labels the topological sector, and the Lorentz indices are suppressed. The summation as well as the path integral over $A^{(k)}$ follow from the trace operation. Physical quantities such as $\langle E_{\rm ind}\rangle$ and χ_E can thus be calculated by differentiating with respect to the source $E^{\rm M}_{\rm ext}$. As demonstrated in Sec. III, we expect the topological contribution to decouple from the conventional propagating photons.

In particular, we treat $E^{\rm M}_{\rm ext}$ as a constant classical field (or fixed parameter) that is coupled with E_3. The (cross) term in the (Minkowski) action that will contribute nontrivially to the final topological action takes the following form:

$$iS^{\rm M}_c = i\int dt \int d^3x E^{\rm M}_3 E^{\rm M}_{\rm ext}. \tag{A13}$$

Performing a Wick rotation, we get

$$i\int d\tau \int d^3x E^{\rm E}_3 E^{\rm M}_{\rm ext}. \tag{A14}$$

One can also analytically continue $E^{\rm M}_{\rm ext}$ in the path integral for the actual computation. Because the topological contribution ultimately decouples from the functional integration, we have

$$\mathcal{Z}_{top} = \sum_{k\in\mathbb{Z}} \exp\left(-\pi^2\eta k^2 + i\frac{2\pi k E^{\rm M}_{\rm ext}}{e\beta L_3} V\beta\right) \tag{A15}$$

$$= \sum_{k\in\mathbb{Z}} \exp(-\pi^2\eta k^2 + i\eta\pi k\theta^M_{\rm eff}), \tag{A16}$$

which is indeed in agreement with (28). Then (32), (33) automatically follow. Note that the partition function is invariant under $\theta^M_{\rm ext} \to -\theta^M_{\rm ext}$ (which corresponds to $k \to -k$).

Another way to understand the same feature of the quantization (33) of the electric field in the Hamiltonian approach is as follows. The large gauge transformations (A5) imply that the combination eA_3L_3 must be treated as a phase ϕ which is an angular variable. At the same time the commutation relation (A3) after integrating over $\int d^3x d^3y$ can be rewritten as follows:

$$\left[\frac{e\hat{A}_3 V}{L_1L_2}, \tilde{E}_3 V\right] = i\frac{e}{L_1L_2} V, \tag{A17}$$

where V is the volume of the system $V = L_1L_2L_3$ and $\tilde{E}_3$ is the operator of the electric field along the z direction. Commutator (A17) can be written in the canonical form

$$[\phi, \tilde{E}_3] = i\frac{e}{L_1L_2}, \qquad \phi \equiv eA_3L_3, \tag{A18}$$

which implies that the operator for the electric field can be represented as follows

$$\tilde{E}_3 = -i\left(\frac{e}{L_1L_2}\right)\frac{\partial}{\partial\phi}, \tag{A19}$$

similar to angular momentum operator l_3. The corresponding eigenfunctions have the form $\sim\exp(im\phi)$, while the eigenvalues for the electric field are

$$L_1L_2\tilde{E}_3 = em, \tag{A20}$$

which precisely coincides with quantization (33).

[1] C. Cao, M. van Caspel, and A. R. Zhitnitsky, Topological Casimir effect in Maxwell electrodynamics on a compact manifold, Phys. Rev. D **87**, 105012 (2013).

[2] A. R. Zhitnitsky, Maxwell theory on a compact manifold as a topologically ordered system, Phys. Rev. D **88**, 105029 (2013).

[3] A. R. Zhitnitsky, Topological order and Berry connection for the Maxwell vacuum on a four-torus, Phys. Rev. D **90**, 105007 (2014).

[4] A. R. Zhitnitsky, Dynamical Casimir effect in a small compact manifold for the Maxwell vacuum, Phys. Rev. D **91**, 105027 (2015).

[5] H. B. G. Casimir, On the attraction between two perfectly conducting plates, Proc. K. Ned. Akad. Wet. **51**, 793 (1948).

[6] G. Y. Cho and J. E. Moore, Topological BF field theory description of topological insulators, Ann. Phys. (Amsterdam) **326**, 1515 (2011).

[7] X.-G. Wen, Topological order: From long-range entangled quantum matter to an unification of light and electrons, ISRN Condens. Matter Phys. **2013**, 198710 (2013).

[8] S. Sachdev, The quantum phases of matter, arXiv:1203.4565.

[9] A. Cortijo, F. Guinea, and M. A. H. Vozmediano, Geometrical and topological aspects of graphene and related materials, J. Phys. A **45**, 383001 (2012).

[10] G. E. Volovik, Topology of quantum vacuum, Lect. Notes Phys. **870**, 343 (2013).

[11] G. T. Moore, Quantum theory of the electromagnetic field in a variable-length one-dimensional cavity , J. Math. Phys. (N.Y.) **11**, 2679 (1970); S. A. Fulling and P. C. W. Davies, Radiation from a moving mirror in two dimensional space-time: conformal anomaly, Proc. R. Soc. A **348**, 393 (1976); P. C. Davies and S. A. Fulling, Radiation from moving mirrors and from black holes, Proc. R. Soc. A **356**, 237 (1977).

[12] G. Barton and C. Eberlein, On quantum radiation from a moving body with finite refractive index, Ann. Phys. (N.Y.) **227**, 222 (1993); M. Kardar, and R. Golestanian, The "friction" of vacuum, and other fluctuation-induced forces, Rev. Mod. Phys. **71**, 1233 (1999); V. V. Dodonov, in *Modern Nonlinear Optics*, Part 3, edited by M. W. Evans, I. Prigogine, and S. A. Rice, *Advances in Chemical Physics* Vol. 119 (Wiley, New York, 2001), p. 309.

[13] C. M. Wilson, G. Johansson, A. Pourkabirian, M. Simoen, J. R. Johansson, T. Duty, F. Nori, and P. Delsing, Observation of the dynamical Casimir effect in a superconducting circuit, Nature (London) **479**, 376 (2011); P. Lahteenmaki, G. S. Paraoanu, J. Hassel, and P. J. Hakonen, Dynamical Casimir effect in a Josephson metamaterial, Proc. Natl. Acad. Sci. U.S.A. **110**, 4234 (2013).

[14] I. Sachs and A. Wipf, Finite temperature Schwinger model, Helv. Phys. Acta **65**, 652 (1992); Generalized Thirring models, Ann. Phys. (N.Y.) **249**, 380 (1996); S. Azakov, H. Joos, and A. Wipf, Witten-Veneziano relation for the Schwinger model, Phys. Lett. B **479**, 245 (2000); S. Azakov, The Schwinger model on a circle: Relation between path integral and Hamiltonian approaches, Int. J. Mod. Phys. A **21**, 6593 (2006).

[15] E. Thomas and A. R. Zhitnitsky, Topological susceptibility and contact term in QCD: A toy model, Phys. Rev. D **85**, 044039 (2012).

[16] G. Bressi, G. Carugno, R. Onofrio, and G. Ruoso, Measurement of the Casimir Force between Parallel Metallic Surfaces, Phys. Rev. Lett. **88**, 041804 (2002).

[17] S. K. Lamoreaux, Demonstration of the Casimir Force in the 0.6 to 6 μm Range, Phys. Rev. Lett. **78**, 5 (1997).

[18] V. Chandrasekhar, R. A. Webb, M. J. Brady, M. B. Ketchen, W. J. Gallagher, and A. Kleinsasser, Magnetic Response of a Single, Isolated Gold Loop, Phys. Rev. Lett. **67**, 3578 (1991).

[19] Y. Imry, *Introduction to Mesoscopic Physics*, 2nd ed. (Oxford University Press, New York, 2008); E. Akkermans and G. Montambaux, *Mesoscopic Physics of Electrons and Photons* (Cambridge University Press, Cambridge, England, 2011); W. E. Shanks, Ph.D. thesis, Yale University, 2011.

[20] M. Tsubota, K. Inagaki, T. Matsuura, and S. Tanda, Aharonov-Bohm effect in charge-density wave loops with inherent temporal current switching, Europhys. Lett. **97**, 57011 (2012).

[21] A. R. Zhitnitsky, Inflaton as an auxiliary topological field in a QCD-like system, Phys. Rev. D **89**, 063529 (2014).

[22] A. R. Zhitnitsky, Dynamical de Sitter phase and nontrivial holonomy in strongly coupled gauge theories in an expanding universe, Phys. Rev. D **92**, 043512 (2015).